Can Electrophilicity Act as a Measure of the Redox Potential of First-Row Transition Metal Ions?

ARTICLE *in* CHEMISTRY - A EUROPEAN JOURNAL · AUGUST 2007

Impact Factor: 5.73 · DOI: 10.1002/chem.200700547 · Source: PubMed

5 AUTHORS, INCLUDING:

Pablo Jaque
Universidad Andrés Bello
51 PUBLICATIONS **993** CITATIONS
SEE PROFILE

Paul Geerlings
Vrije Universiteit Brussel
460 PUBLICATIONS **11,506** CITATIONS
SEE PROFILE

DOI: 10.1002/chem.200700547

Can Electrophilicity Act as a Measure of the Redox Potential of First-Row Transition Metal Ions?

Jan Moens,[a] Goedele Roos,[a, c, d] Pablo Jaque,[a, b] Frank De Proft,[a] and Paul Geerlings*[a]

Abstract: Previous contributions concerning the computational approach to redox chemistry have made use of thermodynamic cycles and Car–Parrinello molecular dynamics simulations to obtain accurate redox potential values, whereas this article adopts a conceptual density functional theory (DFT) approach. Conceptual DFT descriptors have found widespread use in the study of thermodynamic and kinetic aspects of a variety of organic and inorganic reactions. However, redox reactions have not received much attention until now. In this contribution, we prove the usefulness of global and local electrophilicity descriptors for the prediction of the redox characteristics of first row transition metal ions (from $Sc^{3+}|Sc^{2+}$ to $Cu^{3+}|Cu^{2+}$) and introduce a scaled definition of the electrophilicity based on the number of electrons an electrophile ideally accepts. This scaled electrophilicity concept acts as a good quantitative estimate of the redox potential. We also identify the first solvation sphere together with the metal ion as the primary active region during the electron uptake process, whereas the second solvation sphere functions as a non-reactive continuum region.

Keywords: density functional calculations · electrophilicity · redox chemistry · theoretical chemistry · transition metals

Introduction

Chemistry deals with an astonishing amount of experimental data that concerns the properties and reactions of millions of compounds and an enormous amount of effort has been devoted to introducing concepts and principles to interpret this avalanche of information. Concepts such as electronegativity, hardness, and softness have become cornerstones in this field of structure and reactivity. These widespread concepts, however, are rather vaguely defined. Conceptual density functional theory (DFT) has provided a theoretical framework in which sharp definitions of these concepts are proposed,[1,2] thereby ensuring their computability and their quantitative use when applied to principles and rules governing the thermodynamic and kinetic aspects of a variety of organic and inorganic reactions. A closer look at the reaction types studied in the past[3] shows the prevalence of generalized acid/base reactions and fundamental types of organic reactions (addition; elimination; and substitution involving electrophilic, nucleophilic and radical reagents) in which the hard/soft acid/base principle[4] plays a fundamental role. Remarkably, however, redox reactions have not received much attention to date despite the fact that they are archetypal reactions that involve a change in the number of electrons, which is one of the basic variables, together with the external potential, in the perturbational approach to chemical reactivity.

The chemical potential (μ) and the chemical hardness (η), defined as the first- and second-order change in energy with respect to the number of electrons, N, respectively, are useful tools for describing the ability of a system to soak up electrons. The electrophilicity index, ω, recently introduced by Parr et al.,[5] combines both descriptors and acts as a measure of the electrophilic power of a reactant. We have used this index as an appropriate descriptor of the one-electron reduction reaction in our efforts to link conceptual DFT to electrochemistry. A previous contribution from our

[a] J. Moens, Dr. G. Roos, Dr. P. Jaque, Prof. Dr. F. De Proft, Prof. Dr. P. Geerlings
Eenheid Algemene Chemie, Faculteit Wetenschappen
Vrije Universiteit Brussel (VUB)
Pleinlaan 2, Brussels (Belgium)
Fax: (+32) 2-629-3317
E-mail: pgeerlin@vub.ac.be

[b] Dr. P. Jaque
Laboratorio de Química Teórica Computacional (QTC)
Facultad de Química
Pontificia Universidad Católica de Chile
Casilla 306, Correo 22, Santiago (Chile)

[c] Dr. G. Roos
Department of Molecular and Cellular Interactions, VIB
1050 Brussels (Belgium)

[d] Dr. G. Roos
Ultrastructure Laboratory
Vrije Universiteit Brussel (VUB), (Belgium)

group in this context[6] uses a complete family of descriptors, namely, the electrophilicity, nucleofugality, and electrofugality,[7] to describe the redox process of a group of oxo acids. This methodology proved to be very successful in resolving trends in the redox potential for the different groups of oxo acids.

Our aim in this paper is to describe the usefulness of global and local electrophilicity values for the prediction of the redox characteristics of first row transition metal ions. By convention, the redox potential measures the tendency of a chemical species in aqueous solution to acquire electrons, as shown in Equation (1):

$$\mathrm{Ox(aq)} + n\,\mathrm{e}^- \rightarrow \mathrm{Red(aq)} \tag{1}$$

in which Ox refers to the oxidized species and Red to the reduced species in solution. In this paper we are interested in the one-electron reduction of a trivalent transition metal ion, in other words the $M^{3+}(aq)|M^{2+}(aq)$ redox couple. Previous contributions that concern the redox chemistry of first row transition metal ions have made use of a thermodynamic cycle that links the process in the gas phase with the solution process.[8,9] As these metal ions remain charged and in solution during the reduction reaction, it is unnecessary to model the electrode surface and it can simply be replaced by a fictitious electron reservoir with a chemical potential of zero, which is appropriate in the context of the electrophilicity descriptor. Since redox reactions are processes that take place in a solvent, the influence of the environment has to be taken into account. As discussed in previous contributions by Li et al. [8] and Uudsemaa and Tamm,[9] the first and second solvation spheres around the transition metal ion are necessary to model the environment correctly. A combination of an explicit first and/or second solvation sphere with a dielectric continuum model (PCM) should provide an appropriate simulation of the solvent.

Theoretical Background

Electrophilicity: As recently defined by Parr et al.,[5] the electrophilicity encompasses the decrease in energy associated with a process of maximum electron uptake between a ligand and a perfect electron donor. They proposed a rigid thermodynamic interpretation of the electrophilicity as a validation of a qualitative suggestion made by Maynard et al.[10] On the basis of a second-order model for the variation of the energy versus the change in the number of electrons (ΔN) with constant external potential ($\nu(\boldsymbol{r})$), that is, the potential due to the nuclei, the energy change is given by Equation (2):

$$\Delta E = \mu\Delta N + \frac{1}{2}\eta(\Delta N)^2 \tag{2}$$

in which the chemical potential (μ) and the chemical hardness (η) are defined by $\mu = \left(\frac{\partial E}{\partial N}\right)_\nu$ and $\eta = \left(\frac{\partial^2 E}{\partial N^2}\right)_\nu$. The system will become saturated with electrons when $\Delta E/\Delta N$ equals zero. The corresponding gain in energy, given by Equation (3), has been identified as the electrophilicity (ω) of the system, which is given by Equation (4):

$$\Delta E = -\frac{\mu^2}{2\eta} \tag{3}$$

$$\omega = \frac{\mu^2}{2\eta} \tag{4}$$

In a finite difference approximation, substituting μ with $-\left(\frac{I+A}{2}\right)$ and η with $I-A$ gives Equation (5) in which I and A are the ionization potential and the electron affinity, respectively.

$$\omega = \frac{(I+A)^2}{8(I-A)} \tag{5}$$

The electrophilicity takes into account the tendency of the system to acquire an additional amount of electrons from the environment with the factor μ^2, whereas the chemical hardness is a measure of the resistance of the system to charge transfer. The charge ($\Delta q_{\mathrm{ideal}}$) that the system carries when it reaches maximum stabilisation is determined by the ratio of the chemical potential and the hardness given in Equation (6):

$$\Delta q_{\mathrm{ideal}} = \frac{\mu}{\eta} = -\frac{I+A}{2(I-A)} \tag{6}$$

Local descriptors: Local descriptors of reactivity have been proposed to describe the site selectivity in a molecule instead of considering the molecule as a whole. The Fukui function $f(\underline{r})$,[11] for example, which measures the sensitivity of the chemical potential of a system to an external perturbation at a particular site, is one of the most popular local reactivity descriptors [Eq. (7)].

$$f(\underline{r}) = \left(\frac{\delta\mu}{\delta\nu(\underline{r})}\right)_N = \left(\frac{\partial\rho(\underline{r})}{\partial N}\right)_{\nu(\underline{r})} \tag{7}$$

Fukui functions for the attack of an electrophile or nucleophile can be defined by using left and right derivatives with respect to the number of electrons. To describe the reactivity of an atom in a molecule it is necessary to condense the value of $f(\underline{r})$ around each atomic site into a single value that quantifies the contribution of that site to the whole molecule. The condensed-to-atom variants of these descriptors for the atomic site k of a molecule are defined by using electron populations (p_k) based on a finite difference approximation of Equation (7),[12] which for a nucleophilic attack gives Equation (8).

$$f_k^+(\underline{r}) = p_k(N+1) - p_k(N) \tag{8}$$

Equation (8) is used in this article as a working equation for the Fukui function to describe a nucleophilic attack. It is

possible to define a local version of the electrophilicity for a nucleophilic attack[13] associated with a site k in a molecule by using f_k^+, which is calculated by using Equation (9):

$$\omega_k^+ = \omega f_k^+ \quad (9)$$

Equation (9) indicates that the maximum electrophilicity power in a molecule will develop at the site that corresponds to the maximum value of f_k^+. Previous studies have shown that the local electrophilicity is a reliable descriptor for predicting intermolecular[14–16] and intramolecular,[15,17] reactivity trends.

Group philicity: In line with our previous interest in the description of group properties through DFT-based descriptors,[18] the group philicity[19] concept is used in this paper. Group philicity is defined as the sum of the condensed local electrophilicity over the atoms coordinated to the reactive atom. It takes the form shown in Equation (10) when expressed in terms of local electrophilicity values for nucleophilic attack.

$$\omega_g^+ = \sum_{k=1}^{n} \omega_k^+ \quad (10)$$

in which n is the number of atoms coordinated to the reactive atom, ω^+_k is the local electrophilicity for nucleophilic attack condensed on atom k and ω^+_g is obtained by adding the local philicity values of the atoms that make up the "group". This descriptor has been shown to be very useful for resolving intermolecular trends in carbonyl[19] derivatives, for example, and the prediction of pK_a values.[20]

Solvent effects: Pérez et al.[21] have examined the effect of solvent on the electrophilicity index by considering the first-order finite variation of ω, expressed as $\Delta\omega$ [Eq. (11)], that is induced by a change from the gas to the solution phase and characterised by the dielectric constant ε of the solvent.

$$\Delta\omega(1 \rightarrow \varepsilon) = \left(\frac{\mu}{\eta}\right)\Delta\mu - \frac{1}{2}\left(\frac{\mu}{\eta}\right)^2 \Delta\eta = \Delta\omega^{(1)} + \Delta\omega^{(2)} \quad (11)$$

The terms $\Delta\mu$ and $\Delta\eta$ describe the variation in μ and η, respectively, when the system goes from the gas phase to solution. They have shown the existence of a linear relationship between the change in electrophilicity and the solvation energy for a series of neutral and electrophilic ligands, see Equation (12):

$$\Delta\omega(1 \rightarrow \varepsilon) = \left(2 + \frac{\Delta N_{max}}{\Delta N}\right)\Delta E_{solv} = \gamma \Delta E_{solv} \quad (12)$$

in which ΔN_{max} corresponds to the maximum amount of electron transfer from the environment (and is therefore the negative of the value of Δq_{ideal}), ΔN is the change in the number of electrons and ΔE_{solv} the change in the solvation energy.

Methodology

Studied structures: We have studied nine of the ten first-row transition metals (Sc–Cu), all of which present an $M^{3+}|M^{2+}$ redox couple. The Zn atom is not included in this study because the Zn^{3+} cation is not found in aqueous solutions, and therefore, experimental data concerning its redox potential are not available. A major advantage of the first row transition metal ions is that relativistic effects can be discarded when describing these systems. Structural data for these metal ions coupled with a discrete first and/or second solvation sphere are available in the literature.[9] These structures were used as the starting geometries for our calculations. Table 1 gives an overview of the different transition metal ions used in this article along with their corresponding experimental redox potentials.

Table 1. Experimental redox potentials for the series of transition metal ions studied.

Redox couple	E°[a] [V]
$Sc^{3+}\|Sc^{2+}$	−2.3[43c]
$Ti^{3+}\|Ti^{2+}$	−0.9[43c,d]
$V^{3+}\|V^{2+}$	−0.255[43a–d]
$Cr^{3+}\|Cr^{2+}$	−0.42[43c]
$Mn^{3+}\|Mn^{2+}$	1.54[43d]
$Fe^{3+}\|Fe^{2+}$	0.77[43b–d]
$Co^{3+}\|Co^{2+}$	1.92[43b–d]
$Ni^{3+}\|Ni^{2+}$	2.3[43c]
$Cu^{3+}\|Cu^{2+}$	2.4[43c,d]

[a] Experimental values.

An in-depth discussion of the values of these experimental redox potentials has been given by Uudsemaa and Tamm.[9] It is worth noting that some of these values have significant experimental uncertainties, for example, the redox couples of $Sc^{3+}|Sc^{2+}$, $Ni^{3+}|Ni^{2+}$, and $Cu^{3+}|Cu^{2+}$, and this must be kept in mind when evaluating correlations between calculated electrophilicity values and redox potentials.

Electrochemical reactions are highly dependent on the environment, therefore, it is important to adequately take the solvent into account.[8] Experimental evidence confirms that ions of the fourth row are not present as bare atoms in water, but are instead octahedrally coordinated.[22] Therefore, we included six discrete water molecules, which form the first solvation sphere, in the quantum chemical calculation. These water molecules are oriented such that their oxygen atoms point towards the central metal ion (see Figure 1a). This octahedron was further expanded by a secondary solvation sphere of 12 water molecules, each of which is linked through hydrogen bonds to the hydrogen atoms of the water molecules in the first solvation sphere (see Figure 1b).

Experimental evidence[23] and molecular simulation analyses[24] support the fact that the second solvation layer is composed of 12 water molecules, although their arrangement is uncertain. As noted by Uudsemaa and Tamm,[25] different

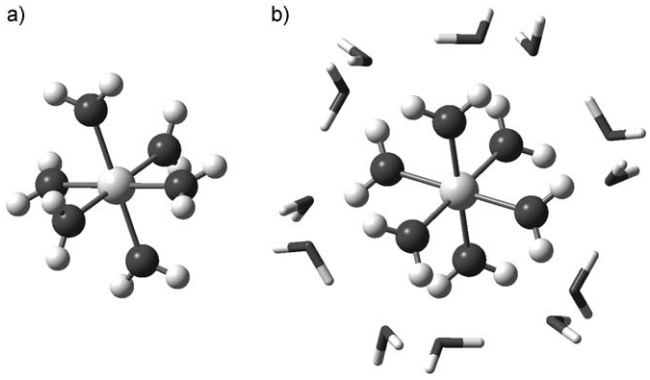

Figure 1. a) The octahedral coordination of the metal ion with six water molecules. b) A dodecahedral representation of the first and second solvation spheres. Six of the eighteen water molecules form an octahedron.

possible minima exist on the potential energy surface, although one type of structure seems to be the lowest in energy, namely that built up from two sets of nine water molecules interacting on two parallel planes. This structure resembles a regular dodecahedron of water molecules in which six of the water molecules lie in the first rather than the second coordination shell of water molecules.[26]

Spin multiplicity of transition metal ions: The octahedral surrounding of the central metal ion results in an energy split that divides the d orbitals into doubly degenerate e_g orbitals and triply degenerate t_{2g} orbitals.[27] The energy separation between these orbitals, which is the ligand-field splitting parameter Δ_O, is dependent on the type of ligands that surround the central metal ion.[27] As shown by the Tsuchida spectrochemical series, the water molecule is intermediate between ligands that result in high- and low-spin cases, therefore, we studied both the high- and low-spin states of every transition metal ion.

The applicability of the electrophilicity descriptor: The electrophilicity descriptor can be considered as the electron affinity combined with an extra term developed by Ayers et al. known as the nucleofugality, which is calculated by using Equation (13):[7]

$$\omega = A + \frac{(I-3A)^2}{8(I-A)} \tag{13}$$

This nucleofugality term increases in importance when the ionisation energy (I) differs significantly from three times the electron affinity (A). As this term has a positive energy contribution, the electrophilicity always overestimates the energy change during the uptake of one electron when considered in a field of constant external potential. In the past, the existence of a linear relationship between the electrophilicity and the electron affinity was shown to exist only for values of Δq_{ideal} that are less negative than -1.[5] The ω descriptor possesses some major advantages relative to the vertical electron affinity. Firstly, it contains the electron affinity and also carries some extra information about the polarisability of the system through the softness factor $1/(I-A)$. Secondly, the local derivatives of this descriptor offer the opportunity to study the reactive site that is prone to electron uptake whilst also taking into account the properties of the global molecule. In the particular situation in which the ionisation energy (I) equals three times the electron affinity (A) then the nucleofugality term becomes zero and ω and A are equal. This situation corresponds to a system with a Δq_{ideal} value of -1 (see Figure 2).

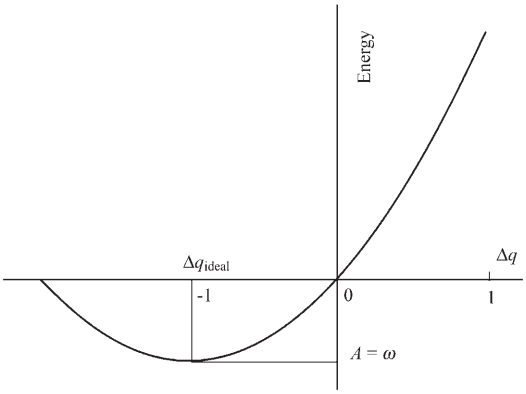

Figure 2. The quadratic model for the dependence of the energy on the molecular charge Δq for the case in which Δq_{ideal} is equal to -1.

As the metal ions in our study are triply charged and highly prone to electron uptake, the values for Δq_{ideal} are much more negative than -1. Therefore, it seems awkward that the energy difference between $q+\Delta q_{ideal}$ and the q charged state is used to describe the one-electron reduction reaction. In this paper we propose a slightly modified definition of the electrophilicity that correctly scales down the original equation for ω [see Eq. (4)] through Δq_{ideal}. It is our aim to approximate the redox potential by using this scaled definition. One could criticize the applicability of the electrophilicity as an approximation of the redox potential when considering the more obvious alternatives, such as the adiabatic ionisation potential. However, the electrophilicity descriptor confines the characteristics of the trivalent metal ion that undergoes the reduction reaction by the vertical electron affinity and ionisation potential of this species. Its local counterpart in terms of the Fukui function offers us a way to interpret the influence of solvent on the redox behaviour of the central metal ion and provides us with a clear image of the stabilising and reductive centres in the global complex. In the discussion of the results that follows, our approach will be compared with redox potential values calculated from the adiabatic ionisation potential coupled with a thermodynamic cycle.

The introduction of Δq_{ideal} in this discussion follows quite naturally from the quadratic model of the energy change versus the charge (Figure 2). As this curve is determined in terms of the chemical potential μ and the chemical hardness η, it is also possible to define it in terms of ω and Δq_{ideal}.

One could imagine a hypothetical situation in which two systems possess the same electrophilicity, therefore, the inclusion of the Δq_{ideal} value for the description of the one-electron uptake process offers the opportunity to differentiate between their electrophilic powers. We will discuss two possible situations in which Δq_{ideal} is less or more negative than -1.

Situation in which $\Delta q_{ideal} \leq -1$: In this case, the molecule readily accepts more than one electron since the value of Δq_{ideal} is more negative than -1. In the hypothesis of two species **1** and **2**, which possess the same electrophilicity, the species with the least negative value of Δq_{ideal} shows the largest energy change during the one-electron uptake process (see Figure 3). To differentiate between the two species,

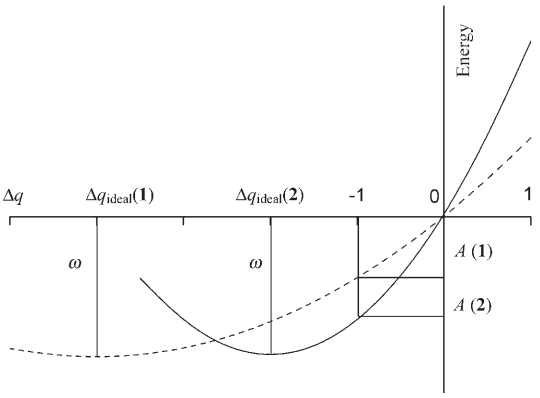

Figure 3. The quadratic model for the dependency of the energy on the molecular charge (Δq) when Δq_{ideal} is more negative than -1 for species **1** (-----) and **2** (——), which possess the same electrophilicity. System **2**, with the least negative Δq_{ideal} value, has the highest energy change, which corresponds to a one-electron uptake process (when Δq equals -1).

the original definition of the electrophilicity was made inversely proportional to $-\Delta q_{\text{ideal}}$. A more negative value of Δq_{ideal} corresponds to a species that is less able to accept one electron. However, a simple division of the original definition of the electrophilicity by the Δq_{ideal} term is unacceptable because it results in the expression of the chemical potential. We therefore introduced a new term $(p-\Delta q_{\text{ideal}})$ in the denominator. After examining the proportionality between ω_{scaled} and the electron affinity A for a series of different Δq_{ideal} values, it turned out that this proportionality can differ significantly for different Δq_{ideal} values and depends on the term p. This large discrepancy in the proportionality hampers comparison between different systems. The smallest discrepancy in the proportionality between A and ω_{scaled} was observed for the different Δq_{ideal} values in the specific case in which p has a value of one.

As a result, the equation for ω_{scaled} has the form shown in Equation (14):

$$\omega_{\text{scaled}} = \frac{2\omega_{\text{Eq.(4)}}}{1-\Delta q_{\text{ideal}}} \tag{14}$$

in which $\omega_{\text{Eq.(4)}}$ is the electrophilicity calculated from Equation (4). The number two in the nominator is chosen so that when Δq_{ideal} is -1 the electrophilicity values calculated by the scaled and original definitions [Eq. (4)] converge. The definition of ω_{scaled} is able to differentiate between the electrophilic powers of two species with the same value of $\omega_{\text{Eq.(4)}}$ by using the Δq_{ideal} term. The derivative of Equation (14) to Δq_{ideal} contains a positive value at constant $\omega_{\text{Eq.(4)}}$. This shows that species with less negative values of Δq_{ideal} have higher values for ω_{scaled} [Eq. (15)].

$$\left(\frac{\partial \omega_{\text{scaled}}}{\partial \Delta q_{\text{ideal}}}\right)_{\omega_{\text{Eq.(4)}}} = \frac{2\omega_{\text{Eq.(4)}}}{(1-\Delta q_{\text{ideal}})^2} > 0 \tag{15}$$

When expressed in terms of the ionisation energy (I) and electron affinity (A), Equation (14) has the form shown in Equation (16):

$$\omega_{\text{scaled}} = \frac{(I+A)^2}{2(3I-A)} \tag{16}$$

in which the denominator is larger than its counterpart in the original electrophilicity equation $(2(3I-A) > 8(I-A))$ [see Eq. (5)]. It follows from this inequality that the ionisation energy is smaller than three times the electron affinity. This corresponds to the situation in which the values for Δq_{ideal} are more negative than -1.

Situation in which $\Delta q_{ideal} \geq -1$: In the case in which Δq_{ideal} is less negative than -1, the system is energetically more favourable when it acquires a charge $q+\Delta q_{\text{ideal}}$ because this means that it will be forced to take up the remaining negative charge (see Figure 4). Considering again systems with the same electrophilicity **1** and **2**, it is now the system with the least negative value of Δq_{ideal} that possesses the lowest electrophilic power. With respect to the first case, $\omega_{\text{Eq.(4)}}$ is now made inversely proportional to $p+\Delta q_{\text{ideal}}$ and a less negative value of Δq_{ideal} corresponds to a species that is less

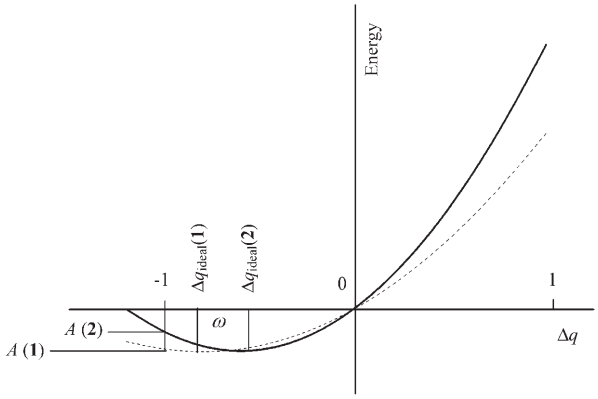

Figure 4. The quadratic model for the dependence of the energy on the molecular charge (Δq) when Δq_{ideal} is less negative than -1 for species **1** (-----) and **2** (——). Species **1**, with the most negative Δq_{ideal} value, also has the highest energy change, which corresponds to a one-electron uptake process (when Δq equals -1).

able to accept a whole electron. The most appropriate value of p was 2 for a series of Δq_{ideal} values less negative than -1.

The scaled formula we propose for the electrophilicity is now shown in Equation (17):

$$\omega_{scaled} = \frac{\omega_{Eq.(4)}}{(2 + \Delta q_{ideal})} \quad (17)$$

in which the Δq_{ideal} term in the denominator has the opposite effect on the value of the electrophilicity than in the previous case. The origin of the $1/(2+\Delta q_{ideal})$ term can be seen by analogy with the previous discussion for the situation in which Δq_{ideal} is more negative than -1. The derivative of Equation (17) to Δq_{ideal} contains a negative value at constant $\omega_{Eq.(4)}$. This indicates that species with more negative values of Δq_{ideal} have higher values of ω_{scaled} [Eq. (18)].

$$\left(\frac{\partial \omega_{scaled}}{\partial \Delta q_{ideal}}\right)_{\omega_{Eq.(4)}} = \frac{-\omega_{Eq.(4)}}{(2 + \Delta q_{ideal})^2} < 0 \quad (18)$$

The denominator must also be larger in this case than the one in the original equation of the electrophilicity because we have scaled down the electrophilicity value [Eq. (19)], which is true when the ionisation energy is larger than three times the electron affinity. This situation corresponds to values Δq_{ideal} that are less negative than -1.

$$\omega_{scaled} = \frac{(I + A)^2}{4(3I - 5A)} \quad (19)$$

Equations (14) and (17) introduced above describe the whole spectrum of Δq_{ideal} values in a continuous way. Both equations coincide for a Δq_{ideal} value of -1, a result we obtain from the equality between Equation (14) and (17), shown in Equation (20):

$$\frac{\omega_{Eq.(4)}}{(2 + \Delta q_{ideal})} = \frac{2\omega_{Eq.(4)}}{(1 - \Delta q_{ideal})} \rightarrow \Delta q_{ideal} = -1 \quad (20)$$

The ultimate goal of our scaled definition of the electrophilicity is to describe the electrophilic capacity of highly positively charged metal ions in an appropriate manner. In most cases we have to deal with systems for which Δq_{ideal} values are more negative than -1, and therefore, ideally take up more than one electron.

Computational methods

Starting structures for the 6- and 18-water models were built up from recently published coordinates for these models.[9] These structures were re-optimised at the 6-311g(d) level by using the three-parameter fitted hybrid functional (B3LYP).[28] The B3LYP hybrid method performs better than the GGA and the LDA schemes for the distances between main group elements[29] that are found in the ligand structures around the metal ions. The B3LYP functional gives structures for coordinated transition metals that are equally as good as the Becke–Perdew 86 (BP86) functional (a GGA-type functional).[30,31] Previous work has shown that the B3LYP functional is capable of accurately modelling some properties of transition metals, such as structures, frequencies and energetics.[32] An extensive study of the influence of different density functionals and basis sets has shown that hybrid and hybrid meta exchange-correlation functionals provide the most accurate geometry of, and are able to correctly predict the reduction potential for, the $Ru^{3+}|Ru^{2+}$ couple.[33]

Frequency calculations were performed to verify that the structures were actually minima on the potential energy surface. Symmetry breaking was allowed during the optimisation procedure. The remaining solvent was modelled through a polarizable continuum model (PCM)[34] around the optimised gas-phase structures. Local condensed values of electrophilic Fukui functions were calculated by using the natural population analysis method (NPA)[35] to determine the electronic population of the N and $N+1$ systems. The electronic properties, such as the electrophilicity, were expressed in terms of the vertical electron affinities and ionisation energies, which obliged us to calculate the energy of the divalent and tetravalent ions at the geometry of the trivalent cations. All calculations were performed by using the Gaussian 03 software package.[36]

Results and Discussion

High-spin or low-spin states? It is not possible in crystal field theory to say that a particular ligand exerts a strong or a weak ligand field without also considering some properties of the metal ion, such as its nature and its oxidation state.[27] We examined the structures in the high- and low-spin states by performing an energetic analysis and chose the state with the lowest energy. It is not relevant to consider high- and low-spin states for 3d metal ions when less than four or more than eight electrons fill the d orbitals, therefore, high- and low-spin states for the oxidized species are only possible for Mn^{3+}, Fe^{3+}, Co^{3+} and Ni^{3+} ions. The energetic differences between the high- and low-spin structures for the different environments are given in Table 2. The trivalent cations of Mn and Fe are more stable in the high-spin than in the low-spin state. This energetic difference decreases, however, when considering more detailed representations of the environment. Nonetheless, the high-spin states of Mn^{3+} and Fe^{3+} remain lower in energy, and therefore, they will be used in the subsequent discussion. The low-spin states of the Co^{3+} and Ni^{3+} cations are more stable for the 18-water models than their high-spin counterparts. Experimental evidence also confirms that Co^{3+} is present in its low-spin state in solution. As the energetic differences between the high- and low-spin states of Co^{3+} and Ni^{3+} are relatively small when explicit water ligands are included in the cluster

Table 2. Energy difference between high- and low-spin states for Mn^{3+}, Fe^{3+}, Co^{3+}, and Ni^{3+} cations in different representations of the environments.

Oxidized species	$E_{high}-E_{low}$ [kJ mol^{-1}] Bare atom	6 water	18 water
Mn^{3+}	−271.1	−72.2	−41.2
Fe^{3+}	−543.6	−134.3	−72.7
Co^{3+}	−593.3	−8.8	24.6
Ni^{3+}	−293.6	−14.7	0.1

model (between 0.1 and 25 kJ mol^{-1}), both spin states will be studied in the following discussion.

Solvent effects on global reactivity descriptors: The electronic chemical potential (μ) is always negative for the trivalent metal ions in the different models. This ability to take up electrons decreases, however, when considering more explicit water molecules in the cluster model (Table 3). The increase of the chemical potential or decrease of electronegativity (since the electronegativity χ equals $-\mu$) can be explained either by an electronic saturation effect coming from a charge transfer from the solvent molecules to the cation[37] or as a result of a polarization effect induced by the bulk solvent.[21] In contrast to the chemical potential, the chemical hardness diminishes, which results in softer systems and suggests a lower resistance to the exchange of electrons with their environment. The inclusion of more solvent molecules causes an increase in the effective radius (solute radius plus the first or second solvation sphere) of the solute molecule. As a basic inverse proportionality exists between the size of a system and its hardness, the chemical hardness will decrease.[4,38] The value of the electrophilicity decreases with the introduction of explicit water molecules owing to variations in the chemical potential rather than the hardness.

Bringing reagents from a gaseous environment into solution phase ($M^{3+}(g) \rightarrow M^{3+}(aq)$) is characterized by a solvation energy (ΔE_{solv}), which has an effect on the reactivity descriptors of the reagent. Table 3 shows the influence of a dielectric continuum on the values of the chemical potential (μ), the chemical hardness (η) and the electrophilicity ω. Changes in the descriptors through use of the PCM model were calculated as the difference between the values given by this model and those in the gas phase. The solvation energy was measured as the difference between the energy in solution and that in the gas phase.

Placing systems in a dielectric continuum results in lower values of the chemical hardness, and as a result, in softer species with respect to the gas phase. The chemical potential, however, increases upon going from the gas phase to solution.[39] Less significant changes in the chemical potential are observed for the most elaborate representations of the discrete solvent shells. This finding can be explained by considering the charge dependency of the change in the chemical potential, as discussed by Pérez et al.[21]

Since the inclusion of more water shells results in a delocalisation of the charge away from the metal core, the chemical potential decreases less. As previously mentioned, the increase in μ is the main reason for the decrease in the elec-

Table 3. The chemical potential (μ) the chemical hardness (η) and the electrophilicity (ω) in the gas phase (G) and their change in solution ($\Delta\mu$, $\Delta\eta$, $\Delta\omega$) for the 3d metal ions. Values for the solvation energy (ΔE_{solv}) are also reported. All values are given in a.u.[a]

		μ(G)	$\Delta\mu$	η(G)	$\Delta\eta$	ω(G)	$\Delta\omega$	ΔE_{solv}
Sc^{3+}	bare atom	−1.819	0.949	1.767	−0.322	0.936	−0.674	−1.427
	$6H_2O$	−0.686	0.446	0.469	−0.151	0.503	−0.412	−0.696
	$18H_2O$	−0.493	0.303	0.415	−0.113	0.293	−0.234	−0.499
Ti^{3+}	bare atom	−1.325	0.984	0.586	−0.329	1.499	−1.273	−1.483
	$6H_2O$	−0.663	0.452	0.324	−0.153	0.680	−0.550	−0.705
	$18H_2O$	−0.469	0.303	0.288	−0.119	0.382	−0.301	−0.501
V^{3+}	bare atom	−1.419	0.995	0.644	−0.333	1.562	−1.273	−1.497
	$6H_2O$	−0.707	0.456	0.330	−0.167	0.757	−0.564	−0.706
	$18H_2O$	−0.502	0.304	0.308	−0.120	0.409	−0.304	−0.502
Cr^{3+}	bare atom	−1.491	1.034	0.672	−0.346	1.655	−1.334	−1.558
	$6H_2O$	−0.711	0.460	0.393	−0.156	0.643	−0.511	−0.715
	$18H_2O$	−0.497	0.304	0.363	−0.119	0.341	−0.264	−0.503
Mn^{3+}	bare atom	−1.579	1.057	0.659	−0.352	1.891	−1.448	−1.590
	$6H_2O$	−0.747	0.458	0.308	−0.155	0.905	−0.631	−0.712
	$18H_2O$	−0.531	0.303	0.281	−0.114	0.502	−0.346	−0.504
Fe^{3+}	bare atom	−1.592	1.075	0.877	−0.359	1.445	−1.186	−1.616
	$6H_2O$	−0.770	0.457	0.368	−0.154	0.805	−0.576	−0.710
	$18H_2O$	−0.551	0.301	0.302	−0.114	0.503	−0.336	−0.501
Co^{3+} $M=1$	bare atom	−1.666	1.089	0.621	−0.362	2.234	−1.593	−1.641
$M=1$	$6H_2O$	−0.759	0.468	0.345	−0.156	0.834	−0.610	−0.727
$M=1$	$18H_2O$	−0.534	0.305	0.310	−0.119	0.460	−0.323	−0.506
$M=5$	bare atom	−1.564	1.089	0.731	−0.364	1.674	−1.366	−1.639
$M=5$	$6H_2O$	−0.775	0.459	0.275	−0.155	1.093	−0.676	−0.715
$M=5$	$18H_2O$	−0.576	0.303	0.247	−0.116	0.674	−0.388	−0.503
Ni^{3+} $M=2$	bare atom	−1.782	1.105	0.717	−0.368	2.213	−1.558	−1.661
$M=2$	$6H_2O$	−0.805	0.467	0.277	−0.155	1.173	−0.700	−0.726
$M=2$	$18H_2O$	−0.575	0.304	0.239	−0.114	0.691	−0.396	−0.508
$M=4$	bare atom	−1.685	1.105	0.747	−0.368	1.899	−1.456	−1.661
$M=4$	$6H_2O$	−0.801	0.460	0.242	−0.156	1.324	−0.651	−0.715
$M=4$	$18H_2O$	−0.591	0.303	0.228	−0.119	0.765	−0.387	−0.503
Cu^{3+}	bare atom	−1.752	0.896	0.774	−0.299	1.984	−1.213	−1.345
	$6H_2O$	−0.799	0.463	0.269	−0.155	1.185	−0.691	−0.722
	$18H_2O$	−0.583	0.303	0.249	−0.118	0.683	−0.385	−0.505

[a] The values obtained for both spin multiplicity states (M) of Co^{3+} and Ni^{3+} are also quoted.

trophilicity values. The solvation energy also stabilizes the charged species, thereby decreasing the value for the electrophilicity in solution further. The changes in the reactivity descriptors, such as the electrophilicity and η, seem to decrease from the 6-water model to the 18-water model, which suggests that the quality of the solvent description increases.

Relationship between the redox potential and the electrophilicity: The electrophilicity values of the oxidized forms of the transition metal ions, namely, the trivalent species (M^{3+}), were calculated from Equation (4) for the different models of the environment. As mentioned in the Methodology section, a first (six H_2O molecules) and/or a second solvation sphere (which results in a total of 18 H_2O molecules) was explicitly included in combination with a dielectric continuum to model the remaining solvent. High- and low-spin states were considered only for Co^{3+} and Ni^{3+}. The correlation coefficients between the redox potential and the electrophilicity for the different cluster models are given in Table 4.

Table 4. Correlation coefficients between the redox potential and the electrophilicity (ω) and its reciprocal ($-1/\omega$) in the different models considered. The asterisk indicates that low-spin states of Co^{3+} and Ni^{3+} were used instead of their high-spin counterparts.

$R^{2[a]}$	Gas	Continuum	$6H_2O$	$6H_2O$ + continuum	$18H_2O$	$18H_2O$ + continuum
ω	0.76	0.44	0.88	0.76	0.87	0.79
*			0.83	0.73	0.79	0.72
$-1/\omega$	0.68	0.56	0.95	0.96	0.94	0.95
*			0.91	0.91	0.88	0.91

[a] Correlation coefficient.

The explicit consideration of the first and/or second solvation sphere improves the correlation coefficients between the electrophilicity and the redox potential. As the influence of ligands on the chemistry of the transition metal ion is important, an explicit consideration of the solvent molecules is absolutely necessary for a correct description of the system. The continuum solvent model provides an effective alternative to the inclusion of long-range electrostatic interactions, although it fails when only the metal ion is studied owing to the absence of a strong ligand effect. The increase in R^2 values when more discrete solvent molecules and a continuum solvent model are included can be explained by a decrease in the charge of the metal ion, which becomes more delocalised over the different water molecules.

The PCM model works well for neutral systems,[34] whereas highly charged species are difficult to represent in PCM. The inclusion of more discrete solvent molecules results in a delocalisation of the charge on the metal ion to the surrounding water molecules. As a consequence, the PCM model sees a less charged surface of the molecule, which improves the description of the system. Lower correlation coefficients were found when the low-spin states of Ni^{3+} and Co^{3+} were included in the data set instead of their high-spin counterparts because the latter resulted in outliers in the graphs. Uudsemaa and Tamm[9] have reported that the calculated redox potentials of the low-spin states for the $Ni^{3+}|Ni^{2+}$ and $Co^{3+}|Co^{2+}$ couples differ more from the experimental values than the high-spin states. They assigned these discrepancies to the large uncertainties in the experimental values of the redox potentials. However, by using a hyperbolic fitting instead of a linear relationship between the redox potential and the electrophilicity, the R^2 values improve. As a more negative value of $-1/\omega$ is linked to a reagent that is less prone to an electron uptake process (corresponding to a lower ω), the trends in $-1/\omega$ and ω have qualitatively the same meaning, but give quantitatively different results. These findings are summarized in Table 4, which confirms that the hyberbolic fitting improves the correlation coefficients.

Relationship between the redox potential and the scaled version of the electrophilicity: As stated in the Methodology section, we have proposed a modified version of the electrophilicity expression that explicitly takes into account the Δq_{ideal} value.

Validating this equation [Eqs (14) and (17)], we re-examined the relationship between the redox potential and the scaled electrophilicity index (ω_{scaled}). The correlation coefficients obtained are summarised in Table 5.

Table 5. Correlation coefficients between the redox potential and the electrophilicity calculated with the scaled formula for the triply charged metal ions in the different models of the environment. The asterisk indicates that low-spin states of Co^{3+} and Ni^{3+} were used instead of their high-spin counterparts.

R^2	Gas	Continuum	$6H_2O$	$6H_2O$ +continuum	$18H_2O$	$18H_2O$ +continuum
ω_{scaled}	0.83	0.57	0.95	0.95	0.90	0.91
*			0.91	0.90	0.84	0.85

The scaled electrophilicity index gave appreciably better correlations for every model than the original definition of the electrophilicity index (see the section on the Relationship between the redox potential and the electrophilicity and Tables 4 and 5), especially in the cluster that included six water molecules in the gas phase and in solution (Figure 5a and b). This reinforces the idea that the explicit insertion of this value is useful in improving the description of the redox reaction for those systems with highly positively charged ions and a broad spectrum of Δq_{ideal} values. It can be seen from Figure 5b that the electrophilicity calculated from Equation (4) for metal ions that are easily reduced, in other words those that possess a high redox potential, shows larger differences between the ω of the metal ions than their respective redox potentials. Since the original definition of the electrophilicity carries insufficient information in the case of highly positively charged ions, the explicit introduction of Δq_{ideal} values corrects this lack of information. The energy differences between the electron affinity and the electrophilicity are a measure of the overestimation of the

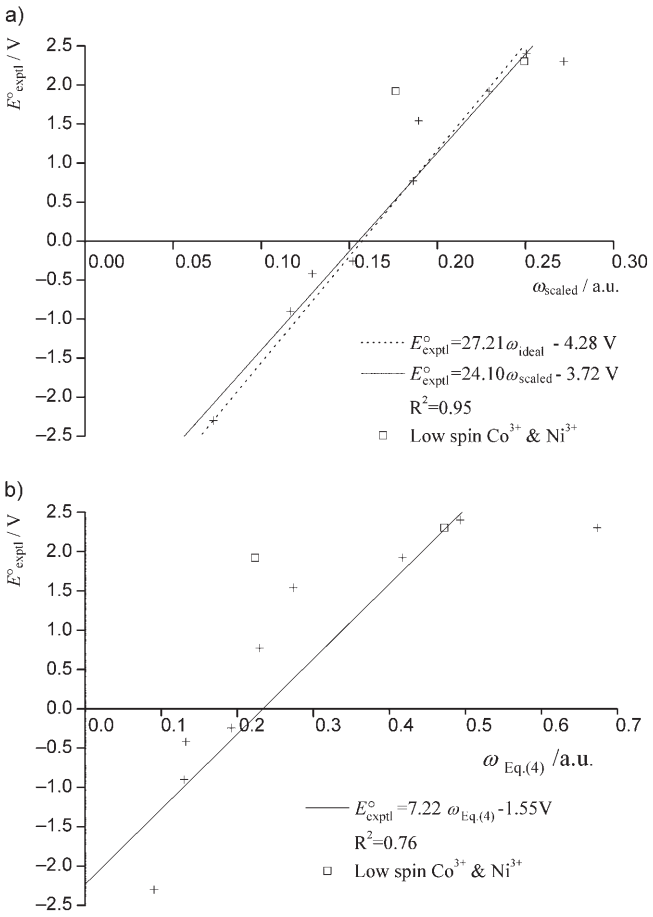

Figure 5. a) A plot of experimental $E°$ values versus ω_{scaled} in the cluster with six water molecules and a solvent model. The ideal line (dotted line) is given for comparison. b) A plot of experimental $E°$ values versus ω calculated by using Equation (4) for the cluster with six water molecules and a solvent model. The results for the low-spin cases of Co^{3+} and Ni^{3+} are shown as squares in both a) and b) and are not incorporated in the correlation.

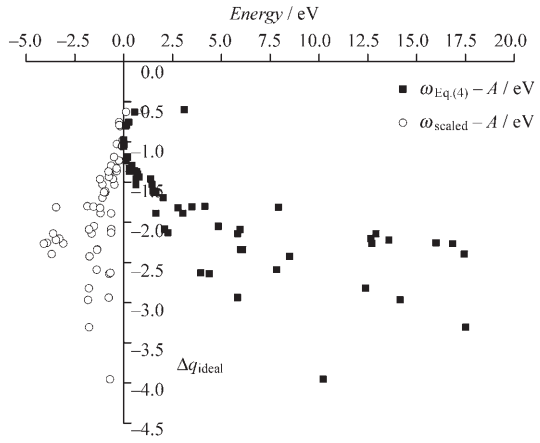

Figure 6. Difference between ω (original (■) and scaled (◇) equations) and the electron affinity, expressed in eV, as a function of the Δq_{ideal} value for species in the gas phase and in solution.

Table 6. Summary of the results for $\omega_{Eq.(4)}$, ω_{scaled}, and Δq_{ideal} versus the redox potential for metal ions in the gas phase, in solution, and in the 6- and 18-water models. (see text for the meaning of [a] and [b]).

	$\omega_{Eq.(4)}$ [a.u.]	Δq_{ideal}	ω_{scaled} [a.u.]	$E°$ [V]
bare atom in gas phase[a]				
Mn^{3+}	1.891	−2.39	1.114	1.54
Ni^{3+} (M = 4)	1.899	−2.25	1.167	2.3
bare atom in PCM[a]				
Mn^{3+}	0.443	−1.70	0.328	1.54
Ni^{3+} (M = 4)	0.444	−1.53	0.351	2.3
6-water model[b]				
Ti^{3+}	0.680	−2.05	0.446	−0.9
Cr^{3+}	0.643	−1.81	0.458	−0.42
6-water model + PCM[a]				
Ti^{3+}	0.130	−1.23	0.117	−0.9
Cr^{3+}	0.133	−1.06	0.129	−0.42
18 water model[a]				
Mn^{3+}	0.502	−1.89	0.347	1.54
Fe^{3+}	0.503	−1.82	0.356	0.77

[a] Almost identical electrophilicity values. [b] Different electrophilicity values.

electrophilicity for the description of the one-electron process. As can be seen from Figure 6, the energy difference between the electrophilicity calculated from the original formula and the electron affinity seems to increase with decreasing values of Δq_{ideal}. The differences are spread out considerably for the same values of Δq_{ideal}, which results in overestimations of between 0 and 18 eV and thereby hampers any meaningful comparisons. The scaled expression for the electrophilicity does a much better job as a measure of the electron affinity by keeping the deviation, which here is an underestimation, small (< 4 eV) and homogeneous.

In some cases the original definition of the electrophilicity yields an incorrect prediction of the relative ability to accept electrons, as shown in Table 6.

For the couples in which the electrophilicity values are almost the same (labelled [a] in Table 6), the electrophilicity is not able to differentiate between these species, and therefore, it is the Δq_{ideal} value that now plays the crucial role, as introduced in the new definition of the electrophilicity. A less negative value of Δq_{ideal} makes species more electrophilic, which corresponds to an increase of the redox potential. The only exception is the last case (Mn^{3+} and Fe^{3+} metal ions), in which the correspondence with the redox potential is broken. In other cases the electrophilicity values of both species are different (labelled [b] in Table 6). The sequence of values obtained with the original definition of the electrophilicity differs from the trend in the redox potential. The scaled definition manages to correct the electrophilicity values.

Identifying the slope as the inverse of the Faraday constant ($1/F = 27.21$ V per a.u. of energy) and the cutoff value as the negative of the standard hydrogen potential (−4.28 V)[33,40,41] it seems possible to use the electrophilicity descriptor to directly measure the redox potential from Figure 5a. As proposed by Parr et al.,[5] the electrophilicity index is based on a thermodynamic interpretation of the energy change of the system after a maximum uptake of electrons, therefore, connecting an electronic property to

the Gibbs free-energy presupposes that entropic and thermal contributions are small. The standard redox potential can be determined from the Nernst equation [Eq. (21)] by calculating the Gibbs free-energy change of the complete redox reaction in which n is the number of exchanged electrons and F is the Faraday constant.

$$E^{\circ}(\text{vs. SHE}) = -\frac{\Delta G^{\circ}}{nF} \tag{21}$$

The calculated value of E° is thus related to the reduction potential of a reference electrode, in this case the standard hydrogen electrode (SHE, $H^{+}(aq)+e^{-}\rightarrow {}^{1}/_{2}H_2(g)$) with an associated free-energy change of -4.28 eV. Equation (19) can be rewritten explicitly in terms of the standard Gibbs free-energy of the reduction reaction of the metal ion (ΔG°_{redox}) and the SHE (ΔG°_{SHE}) in which the number of exchanged electrons n is now one [Eq. (22)].

$$\begin{aligned} E^{\circ}(\text{vs. SHE}) &= -\frac{\Delta G^{\circ}}{nF} \\ &= \frac{-(\Delta G^{\circ}_{redox} - \Delta G^{\circ}_{SHE})}{F} \\ &= -\frac{1}{F}\Delta G^{\circ}_{redox} + \frac{\Delta G^{\circ}_{SHE}}{F} \end{aligned} \tag{22}$$

Equation (22) can be reformulated by approximating ΔG°_{redox} as the negative of the electrophilicity ω ($\Delta G^{\circ}_{redox} \approx -\omega(M^{3+})$) to give Equation (23) in which E°_{abs} is the absolute value of the redox potential, which takes the Gibbs free-energy of the SHE into account explicitly, and E° is the value of the redox potential relative to the absolute half-cell potential of the SHE.

$$E^{\circ} - \frac{\Delta G^{\circ}_{SHE}}{F} = E^{\circ}_{abs} = \frac{\omega}{F} \tag{23}$$

As shown in Figure 7, the correlation coefficient between the scaled electrophilicity (in terms of V) and the absolute redox potential is very high, with a cutoff value of zero for metal ions in a first solvation sphere and a PCM solvent. The introduction of our scaled formula, which explicitly includes Δq_{ideal} values, means that the electrophilicity can act as an appropriate estimation of the one-electron energy change. This is remarkable because the electrophilicity does not contain information about the properties of the reaction product.

The results for ω_{scaled} are listed in Table 7 along with the absolute values of the redox potentials. The difference between the electrophilicity values calculated with the scaled equation and the absolute redox potential are smaller than 0.20 V for five out of the nine metal ions (Sc, V, Fe, high spin Co and Cu). The environment was modelled by a six-water environment accompanied by a dielectric continuum. Although the aim of this article is not so much to obtain an accurate calculation of the redox potential, since other computational procedures based on a thermodynamic cycle[8,9,33,41] and Car–Parrinello molecular dynamics simulations[42] are more suited for this purpose, we nonetheless obtained a reasonably good estimation of the redox potential values.

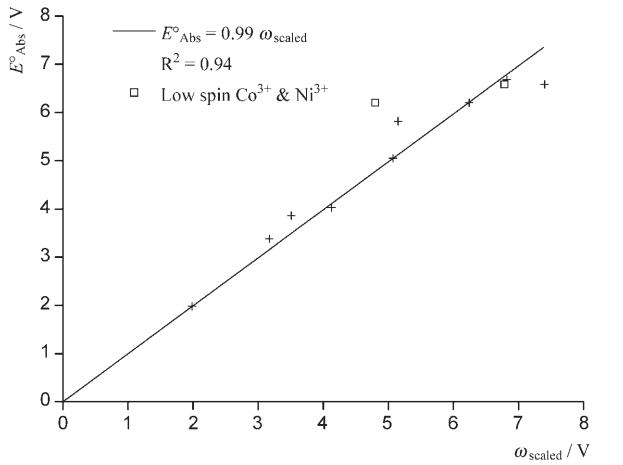

Figure 7. Correlation between the values *of* E°_{abs} and ω_{scaled} for metal ions that are surrounded by six water molecules and a solvent model. The low-spin cases for Co^{3+} and Ni^{3+} are indicated by squares.

Table 7. Values for ω_{scaled} in a six-water model with a dielectric continuum and E° values calculated from a thermodynamic cycle versus the experimental absolute E° values.

	E°_{abs} [a] [V]	ω_{scaled} [V]	E°_{abs} [b] [V] $6H_2O$ + continuum	E°_{abs} [b] [V] $18H_2O$ + continuum
Sc^{3+}	1.98	1.98	2.80	1.86
Ti^{3+}	3.38	3.17	3.87	3.02
V^{3+}	4.02	4.13	4.87	3.76
Cr^{3+}	3.86	3.51	4.54	3.50
Mn^{3+}	5.82	5.15	6.57	5.40
Fe^{3+}	5.05	5.07	6.01	5.06
Co^{3+}	6.20	4.80	7.05	5.97
$M=1$				
Co^{3+}	6.20	6.24	7.23	6.23
$M=5$				
Ni^{3+}	6.58	6.78	8.03	6.78
$M=2$				
Ni^{3+}	6.58	7.40	8.24	6.98
$M=4$				
Cu^{3+}	6.68	6.82	7.94	6.74
MUE[c]		0.26	0.94	0.22
MSE[d]		−0.01	0.94	−0.11

[a] Experimental values. [b] Calculated values. [c] MUE: mean unsigned error calculated for all high-spin complexes. [d] MSE: mean signed error calculated for all high-spin complexes.

Besides the ω_{scaled} values, we also calculated the redox potential by a thermodynamic cycle. Examples of such cycles are numerous in the literature[8,9,33,41] for use in the theoretical prediction of standard reduction potentials. In the study of one-electron reduction reactions a thermodynamic cycle relates the free-energy change in the studied reduction half-reaction (ΔG°_{redox}) to the free-energy change in the gas phase and standard-state solvation free-energies of the oxidised (ΔG°_{solv}(ox)) and reduced species (ΔG°_{solv}(red)).

The expression for the redox potential for one-electron reduction reactions, based on Equation (22), will then become that given by Equation (24):

$$E^{\circ}(\text{vs. SHE}) = -\frac{1}{F}\Delta G^{\circ}_{\text{redox}} + \frac{\Delta G^{\circ}_{\text{SHE}}}{F} = -\frac{1}{F}(-I^{\circ} + \Delta G^{\circ}_{\text{evr}} + \Delta G^{\circ}_{\text{solv}}(\text{red}) - \Delta G^{\circ}_{\text{solv}}(\text{ox})) + \frac{\Delta G^{\circ}_{\text{SHE}}}{F} \quad (24)$$

in which I° is the adiabatic ionisation energy of the reduced species at 0 K and $\Delta G^{\circ}_{\text{evr}}$ is the electronic, vibrational and rotational contribution to the free-energy difference of the reduction reaction in the gas phase. The absolute values of the redox potential calculated by means of a thermodynamic cycle are listed in Table 7. The electrophilicity descriptor in the scaled form seems well capable of predicting and quantifying the redox potential (Table 7). To compare the performance of our approach to the thermodynamic cycle method the potential difference between calculated and experimental redox potential values is given by the mean unsigned error (MUE) and mean signed error (MSE) in Table 7.

The MUE and MSE values show that redox potential values approximated by ω_{scaled}, which were calculated in a cluster of six water molecules surrounded with a continuous solvent, gave better quantitative results than the thermodynamic cycle calculation in a cluster of six water molecules embedded in a continuous solvent. Furthermore, these ω_{scaled} values are almost as accurate as the redox potentials acquired from a thermodynamic cycle approach in an 18-water cluster. One exception is the low-spin state of Co^{3+}, which was also found to be an outlier in the previous discussions.

As stated earlier, one of the advantages of working with the electrophilicity is the possibility of transforming it into a local version through the Fukui function. The local philicity will be thoroughly discussed in the following section.

Local reactivity descriptors: The local philicity is a more powerful concept than the global electrophilicity because the former contains the latter in combination with the site selectivity in the molecule. Instead of studying the whole system, local values of the electrophilicity provide a clear image of the ability of a metal ion to accept electrons. To identify the most reactive site of the global complex, the values of the electrophilicity for nucleophilic attack and charges were calculated for the metal ion and the first and second solvation layer. It can be seen from Table 8 that the charge of the global system is not completely condensed on the metal ion, but instead it is delocalised over the surrounding water molecules, which indicates that some transfer of electron density takes place from the water ligands to the ion. The values for the Fukui functions for nucleophilic attack (f^{+}) (Table 8) and the group philicity ω^{+} (Figure 8a) in the six-water model show that this complex consists of two reactive regions, namely, the central metal ion and the first solvation sphere. If one includes the ω^{+} values condensed on both regions in the description of the redox properties, this will simply lead to the global electrophilicity descriptor in the six-water model. We have already shown the efficiency of this descriptor in relation to the redox potential (see the section on the Relationship between the redox potential and the electrophilicity).

Table 8. Overview of the charge (NPA) and the electrophilic Fukui functions condensed on only the metal ion, only the first, and only the second solvation sphere for the different transition metal ions.

		q_{NPA}			f^{+}		
Bare atom	Solvation model	Bare atom	First sphere	Second sphere	Bare atom	First sphere	Second sphere
Sc^{3+}	$6H_2O$	2.101	0.899		0.650	0.350	
Sc^{3+}	$18H_2O$	2.024	0.382	0.594	0.507	0.174	0.319
Ti^{3+}	$6H_2O$	1.944	1.056		0.551	0.449	
Ti^{3+}	$18H_2O$	1.871	0.524	0.605	0.565	0.286	0.148
V^{3+}	$6H_2O$	1.886	1.114		0.504	0.496	
V^{3+}	$18H_2O$	1.809	0.575	0.617	0.495	0.351	0.154
Cr^{3+}	$6H_2O$	1.876	1.124		0.380	0.620	
Cr^{3+}	$18H_2O$	1.817	0.556	0.627	0.355	0.478	0.167
Mn^{3+}	$6H_2O$	2.030	0.970		0.388	0.612	
Mn^{3+}	$18H_2O$	1.964	0.391	0.645	0.354	0.487	0.159
Fe^{3+}	$6H_2O$	2.146	0.854		0.502	0.498	
Fe^{3+}	$18H_2O$	2.136	0.240	0.625	0.524	0.324	0.152
Co^{3+}							
$M=5$	$6H_2O$	2.036	0.964		0.415	0.585	
$M=5$	$18H_2O$	2.025	0.346	0.629	0.439	0.406	0.154
$M=1$	$6H_2O$	1.676	1.324		0.278	0.722	
$M=1$	$18H_2O$	1.627	0.719	0.654	0.263	0.569	0.169
Ni^{3+}							
$M=4$	$6H_2O$	1.939	1.061		0.335	0.665	
$M=4$	$18H_2O$	1.940	0.420	0.640	0.370	0.470	0.160
$M=2$	$6H_2O$	1.782	1.218		0.217	0.783	
$M=2$	$18H_2O$	1.744	0.578	0.677	0.204	0.616	0.180
Cu^{3+}	$6H_2O$	1.861	1.139		0.243	0.757	
Cu^{3+}	$18H_2O$	1.846	0.480	0.674	0.248	0.571	0.181

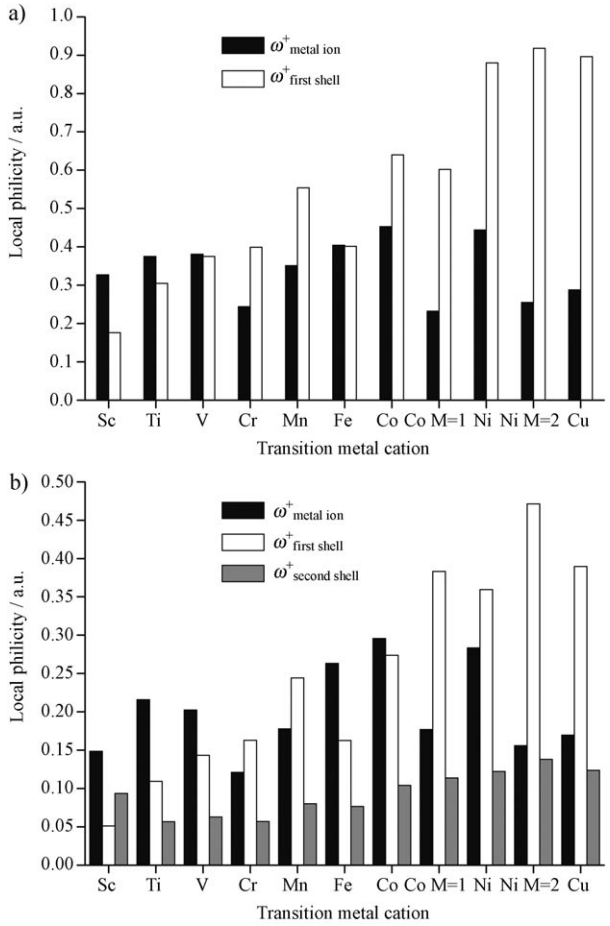

Figure 8. Group ω^+ values condensed on a) the metal ion and the first solvation shell and b) the metal ion and the first and second solvation shells for the different trivalent transition metal ions.

The inclusion of a second solvation sphere to give the 18-water model rearranges the charge of the first solvation sphere, whereas the charge on the metal ion remains nearly constant. Concerning the different metal ions, the charge on the second solvation sphere remains almost constant (except for Sc^{3+}) and is higher than the charge on the first one (except Co^{3+}, which has a multiplicity of one). The values of the charges do not change when molecules are transferred from the gas phase to solvent (PCM). In fact the different solvation layers can be considered as a kind of conductor that provides transfer of an electron through hydrogen bonds towards the central metal ion. The second solvation sphere must attract the electrons from the electrode and pass them efficiently to the central metal ion. The small values of f^+ condensed on the second solvation sphere suggest that a large part of the attracted electron is transferred to the inner core of the complex. In combination with the ω^+ values presented in Figure 8b, these results confirm that the second solvation sphere has only a small influence on the reactivity of the global system and really acts as kind of a continuum.

The combination of the properties of the central metal ion and the first solvation sphere correctly mimics the redox behaviour of the global cluster. The group philicity values of the central metal ion that include the first solvation sphere, given by Equation (25), yield results in relation to the experimental redox potential that are as equally good as the electrophilicity values of the global complex in the 18-water model (see Tables 4 and 9).

$$\omega_g{}^+ = \sum_k^{first\ shell} \omega_k{}^+ + \omega_{metal\ ion}{}^+ \qquad (25)$$

Table 9. Correlation coefficients between group ω^+ and $E°$ for values of ω^+ condensed on the first solvation layer and the metal ion. * Low-spin states of Co^{3+} and Ni^{3+} are used instead of their high-spin counterparts.

R^2	$18H_2O$	$18H_2O+PCM$
$\omega^+{}_g$	0.90	0.80
*	0.83	0.74

This finding confirms that the second solvation sphere has no effect on the reactivity of the transition metal ion. One exception is the Sc^{3+} ion, which possesses higher values of ω^+ on the second solvation sphere than on the first one. Highly reactive domains that possess large values of f^+ on the outside region of the global system, as is the case for the second solvation shell in Sc^{3+}, will make it even more difficult for an electron to reach the inner core of the cluster, therefore, this ion has a lower redox potential.

Conclusions

The global value of the electrophilicity correctly predicts the redox characteristics of transition metal ions in aqueous solution. The explicit inclusion of the aqueous environment by water molecules in a first and second solvation sphere improves the description of the one-electron uptake process. As the electrophilicity contains too little information about the transition of the system from the N to the $N+1$ electrons state in the case of highly positively charged ions, a scaled equation that includes the value of Δq_{ideal} has been introduced. This scaled electrophilicity index has shown its efficiency in resolving trends in the redox potential and acts as a good estimate for redox potential values. Analysis of the local electrophilicity makes it possible to identify different reactive regions of the global metal–aqua complex. This complex is built up from a very reactive first solvation sphere, which acts as an important region during the electron uptake process, whereas the second solvation sphere acts as an electron attracting region that carries the electron to the core region of the metal–aqua complex. The second solvation sphere works as a continuum that does not influence the reactivity of the remaining complex considerably. Trends in the redox potential can therefore be correctly mimicked by using the group philicity of the first solvation sphere and the metal ion.

Acknowledgements

P.G. thanks the Fund for Scientific Research Flanders (FWO) and the VUB for continuous support of his research group. P.J., whose stay in the ALGC group was financed by the Chile–Flanders Bilateral Agreement, also acknowledges FONDECYT (project no. 1060590). J.M. and G.R. thank the Fund for Scientific Research Flanders (FWO) for a predoctoral (Aspirant) fellowship.

[1] P. Hohenberg, W. Kohn, *Phys. Rev.* **1964**, *136*, B864.
[2] R. G. Parr, W. Yang, *Annu. Rev. Phys. Chem.* **1995**, *46*, 701.
[3] P. Geerlings, F. De Proft, W. Langenaeker, *Chem. Rev.* **2003**, *103*, 1793.
[4] R. G. Pearson, *Science* **1966**, *151*, 172.
[5] R. G. Parr, L. V. Szentpály, S. Liu, *J. Am. Chem. Soc.* **1999**, *121*, 1922.
[6] J. Moens, G. Roos, P. Geerlings, *Chem. Eur. J.*, DOI:10.1002/chem.200601896.
[7] P. W. Ayers, J. S. M. Anderson, J. I. Rodriguez, Z. Jawed, *Phys. Chem. Chem. Phys.* **2005**, *7*, 1918.
[8] J. Li, C. L. Fisher, J. Chen, D. Bashford, L. Noodleman, *Inorg. Chem.* **1996**, *35*, 4694.
[9] M. Uudsemaa, T. Tamm, *J. Phys. Chem. A* **2003**, *107*, 9997.
[10] A. T. Maynard, M. Huang, W. G. Rice, D. G. Covell, *Proc. Natl. Acad. Sci. USA* **1998**, *95*, 11578.
[11] R. G. Parr, W. Yang, *J. Am. Chem. Soc.* **1984**, *106*, 4049.
[12] W. Yang, W. J. Mortier, *J. Am. Chem. Soc.* **1986**, *108*, 5708.
[13] P. K. Chattaraj, B. Maiti, U. Sarkar, *J. Phys. Chem. A* **2003**, *107*, 4973.
[14] R. K. Roy, *J. Phys. Chem. A* **2004**, *108*, 4934.
[15] P. K. Chattaraj, U. Sarkar, D. R. Roy, *Chem. Rev.* **2006**, *106*, 2065.
[16] D. R. Roy, R. Parthasarathi, J. Padmanabhan, U. Sarkar, V. Subramanian, P. K. Chattaraj, *J. Phys. Chem. A* **2006**, *110*, 1084.
[17] L. Meneses, W. Tiznado, R. R. Contreras, P. Fuentealba, *Chem. Phys. Lett.* **2004**, *383*, 181.
[18] a) F. De Proft, W. Langenaeker, P. Geerlings, *J. Phys. Chem.* **1993**, *97*, 1826; b) F. De Proft, W. Langenaeker, P. Geerlings, *Tetrahedron* **1995**, *51*, 4021; c) R. Vivas-Reyes, F. De Proft, M. Biesemans, R. Willem, P. Geerlings, *J. Phys. Chem. A* **2002**, *106*, 2753; d) K. T. Giju, F. De Proft, P. Geerlings, *J. Phys. Chem. A* **2005**, *109*, 2925; e) T. Leyssens, P. Geerlings, D. Peeters, *J. Phys. Chem. A* **2005**, *109*, 9882.
[19] R. Parthasarathi, J. Padmanabhan, M. Elango, V. Subramanian, P. K. Chattaraj, *Chem. Phys. Lett.* **2004**, *394*, 225.
[20] R. Parthasarathi, J. Padmanabhan, M. Elango, K. Chitra, V. Subramanian, P. K. Chattaraj, *J. Phys. Chem. A* **2006**, *110*, 6540.
[21] P. Pérez, A. Toro-Labbé, R. Contreras, *J. Am. Chem. Soc.* **2001**, *123*, 5527.
[22] N. N. Greenwood, A. Earnshaw, *Chemistry of the Elements*, Butterworth–Heinmann, Oxford, **1997**.
[23] a) J. Zeng, J. S. Crow, N. S. Hush, J. R. Reimers, *J. Phys. Chem.* **1994**, *98*, 11075; b) E. Clementi, R. Barsotti, R. *Chem. Phys. Lett.* **1978**, *59*, 21; c) T. Radnai, G. Palinkas, G. I. Szasz, K. Z. Heinzinger, *Z. Naturforsch. A* **1987**, *36*, 1076.
[24] H. Ohtaki, T. Radnai, *Chem. Rev.* **1993**, *93*, 1157.
[25] M. Uudsemaa, T. Tamm, *Chem. Phys. Lett.* **2001**, *342*, 667.
[26] G. D. Markham, J. P. Glusker, C. W. Bock, *J. Phys. Chem. B* **2002**, *106*, 5118.
[27] D. F. Shriver, P. W. Atkins, *Inorganic Chemistry*, 3rd ed, Oxford University Press, **1999**.
[28] a) A. D. Becke, *J. Chem. Phys.* **1993**, *98*, 5648; b) C. Lee, W. Yang, R. G. Parr, *Phys. Rev. B* **1988**, *37*, 785.
[29] T. Ziegler, *J. Chem. Soc. Dalton Trans.* **2002**, 642.
[30] W. Koch, M. C. Holthausen, *A Chemist's Guide to Density Functional Theory*, Wiley-VCH, Weinheim, **2000**.
[31] T. Wagener, G. Frenking, *Inorg. Chem.* **1998**, *37*, 1805.
[32] a) G. Frenking, N. Frohlich, *Chem. Rev.* **2000**, *100*, 717; b) P. E. M. Siegbahn, M. R. A. Blomberg, *Chem. Rev.* **2000**, *100*, 421; c) K. P. Jensen, B. O. Roos, U. Ryde, *J. Chem. Phys.* **2007**, *126*, 014103.
[33] P. Jaque, A. V. Marenich, C. J. Cramer, D. G. Truhlar, *J. Phys. Chem. C* **2007**, *111*, 5783.
[34] J. Tomasi, B. Mennucci, R. Cammi, *Chem. Rev.* **2005**, *105*, 2999.
[35] a) A. E. Reed, L. A. Curtis, F. Weinhold, *Chem. Rev.* **1988**, *88*, 899; b) A. E. Reed, R. B. Weinstock, F. Weinhold, *J. Chem. Phys.* **1985**, *83*, 735.
[36] Gaussian 03, Revision B.03, M. J. Frisch, G. W. Trucks, H. B. Schlegel, G. E. Scuseria, M. A. Robb, J. R. Cheeseman, J. A. Montgomery, Jr., T. Vreven, K. N. Kudin, J. C. Burant, J. M. Millam, S. S. Iyengar, J. Tomasi, V. Barone, B. Mennucci, M. Cossi, G. Scalmani, N. Rega, G. A. Petersson, H. Nakatsuji, M. Hada, M. Ehara, K. Toyota, R. Fukuda, J. Hasegawa, M. Ishida, T. Nakajima, Y. Honda, O. Kitao, H. Nakai, M. Klene, X. Li, J. E. Knox, H. P. Hratchian, J. B. Cross, V. Bakken, C. Adamo, J. Jaramillo, R. Gomperts, R. E. Stratmann, O. Yazyev, A. J. Austin, R. Cammi, C. Pomelli, J. W. Ochterski, P. Y. Ayala, K. Morokuma, G. A. Voth, P. Salvador, J. J. Dannenberg, V. G. Zakrzewski, S. Dapprich, A. D. Daniels, M. C. Strain, O. Farkas, D. K. Malick, A. D. Rabuck, K. Raghavachari, J. B. Foresman, J. V. Ortiz, Q. Cui, A. G. Baboul, S. Clifford, J. Cioslowski, B. B. Stefanov, G. Liu, A. Liashenko, P. Piskorz, I. Komaromi, R. L. Martin, D. J. Fox, T. Keith, M. A. Al-Laham, C. Y. Peng, A. Nanayakkara, M. Challacombe, P. M. W. Gill, B. Johnson, W. Chen, M. W. Wong, C. Gonzalez, J. A. Pople, Gaussian, Inc., Wallingford CT, **2004**.
[37] L. Meneses, P. Fuentealba, R. Contreras, *Chem. Phys. Lett.* **2006**, *433*, 54–57.
[38] T. K. Ghanty, S. K. Ghosh, *J. Phys. Chem.* **1993**, *97*, 4951.
[39] a) B. Safi, R. Balawender, P. Geerlings, *J. Phys. Chem. A* **2001**, *105*, 11102; b) R. Balawender, B. Safi, P. Geerlings, *J. Phys. Chem. A* **2001**, *105*, 6703.
[40] C. P. Kelly, C. J. Cramer, D. G. Truhlar, *J. Phys. Chem. B* **2006**, *110*, 16066.
[41] A. Lewis, J. A. Bumpus, D. G. Truhlar, C. J. Cramer, *J. Chem. Educ.* **2004**, *81*, 596.
[42] I. Tavernelli, R. Vuilleumier, M. Sprik, *Phys. Rev. Lett.* **2002**, *88*, 213002.
[43] a) M. S. Antelman, F. J. Harris, *The Encyclopedia of Chemical Electrode Potentials*, Plenum, London, **1982**; b) A. J. Bard, R. Parsons, J. Jordan, *Standard Potentials in Aqueous Solution*; Marcel Dekker, New York, **1985**; c) S. G. Bratsch, *J. Phys. Chem. Ref. Data* **1989**, *18*, 1; d) D. R. Lide, *CRC Handbook of Chemistry and Physics*, CRC Press, Boca Raton, **2002**.

Received: April 6, 2007
Published online: August 31, 2007

